

An in-silico Approach for Recognition of Long non-coding RNA-Associated Competing Endogenous RNA Axes in Prostate Cancer

Mohammad Taheri¹, Arash Safarzadeh², Soudeh Ghafouri-Fard^{2*}, Aria Baniahmad^{1**}

Purpose: Prostate cancer is among the most central sources of cancer-related mortalities. In order to find novel candidates for therapeutic strategies in this kind of cancer, we developed an in-silico method for identification of competing endogenous RNA network.

Methods: According to the microarray data analyses between prostate tumor and normal specimens, we attained 1312 differentially expressed (DE)mRNAs, including 778 down-regulated DEmRNAs (such as CXCL13 and BMP5) and 584 up-regulated DEmRNAs (such as OR51E2 and LUZP2), 39 DElncRNAs, including 10 down-regulated DElncRNAs (such as UBXN10-AS1 and FENDDR) and 29 up-regulated DElncRNAs (such as PCA3 and LINC00992) and 10 DEmiRNAs, including 2 down-regulated DEmiRNAs (such as MIR675 and MIR1908) and 8 up-regulated DEmiRNAs (such as MIR6773 and MIR4683).

Results: We constructed the ceRNA network between these transcripts. We also evaluated the related signaling pathways and the significance of these RNAs in prediction of survival of patients with prostate cancer.

Conclusion: This study provides novel candidates for construction of specific treatment routes for prostate cancer.

Keywords: prostate cancer; ceRNA; lncRNA; miRNA

INTRODUCTION

Long non-coding RNAs (lncRNAs) are a group of transcripts with sizes more than 200 nt. They have diverse regulatory roles in expression of genes. This kind of epigenetic regulators influence epigenetic marks mainly in the nucleus, thus affecting gene transcription⁽¹⁾. In addition, they can serve as molecular sponges for microRNAs (miRNAs)⁽²⁾, thus regulating the expression of miRNA targets. This mode of action leads to establishment of lncRNA/miRNA/mRNA axes that contribute in the several physiological processes. Dysregulation of lncRNAs can lead to several disorders through induction of imbalances in these molecular axes. lncRNAs that act as molecular sponges are called competitive endogenous RNAs (ceRNAs). Evaluation of the activity of ceRNA networks has practical significance, particularly in unraveling the mechanism of carcinogenesis. Prostate cancer as one of the most important sources of cancer-related mortalities⁽³⁾, is one of the hot topics in the field of cancer-related ceRNA networks. For instance, Li et al. have constructed a prostate cancer-specific ceRNA network by incorporating lncRNA/miRNA/mRNA interactions based on experimental and in silico methods. Their method has led to identification of 42 significant prostate cancer-survival-associated triplets which make a condensed sub-network consisting of only 25 nodes. The latter finding shows the involvement of some nodes in many triplets.

MIR22HG/hsa-mir-21/TGFBR2 and MIR22HG/hsa-mir-21/BCL2 triplets have been recognized as two significantly survival-associated triplets with the greatest average degree in the detected subnetwork⁽⁴⁾. Similarly, Guo et al. have constructed a prostate cancer-specific core ceRNA network with the capability to be applied as diagnostic and prognostic marker in this type of cancer⁽⁵⁾.

The current study aimed at identification of the ceRNA network in prostate cancer using an in-silico approach. The related signaling pathways and the significance of these RNAs in prediction of survival of prostate cancer patients have also been evaluated.

MATERIALS AND METHODS

Microarray Data Assessment

The human expression profile of GSE69223, GSE46602, and GSE55945, all with [HG-U133 Plus 2] Affymetrix Human Genome U133 Plus 2.0 Array, which contained 30, 50, and 21 specimens, respectively, were obtained using the Gene Expression Omnibus (GEO; <http://www.ncbi.nlm.nih.gov/geo/>). We chose 15 prostate tumor and 15 normal tissue specimens from GSE69223, 36 prostate tumor samples from GSE46602 and 13 prostate tumor samples from GSE55945 for additional analyses. This data contained lncRNAs, miRNAs and mRNAs expression profile.

Data processing, meta-analysis and evaluation of data

¹Institute of Human Genetics, Jena University Hospital, Jena, Germany.

²Department of Medical Genetics, School of Medicine, Shahid Beheshti University of Medical Sciences, Tehran, Iran.

*Correspondence: Department of Medical Genetics, School of Medicine, Shahid Beheshti University of Medical Sciences, Tehran, Iran. E mail: s.ghafourifard@sbm.ac.ir.

**Institute of Human Genetics, Jena University Hospital, Jena, Germany. E mail: aria.baniahmad@med.uni-jena.de.

Received February 2023 & Accepted May 2023

Table 1. The top 10 up- and downregulated DEmRNAs between prostate tumor and normal samples.

| Down-regulated | | | Up-regulated | | |
|----------------|-----------|-------------------------|--------------|----------|-------------------------|
| DEmRNA | Log FC | Adjusted <i>P</i> value | DEmRNA | Log FC | Adjusted <i>P</i> value |
| CXCL13 | -2.914284 | 0.0001 | OR51E2 | 2.410149 | 0.002 |
| BMP5 | -2.549856 | 0.0002 | LUZP2 | 2.205251 | 0.0005 |
| WIF1 | -2.453527 | 0.0001 | HOXC6 | 2.178773 | 0.0001 |
| NELL2 | -2.383551 | 0.00003 | HPN | 2.004699 | 0.00000002 |
| SLC14A1 | -2.214827 | 0.00004 | C15orf48 | 1.984213 | 0.01 |
| DAPL1 | -2.038041 | 0.002 | TRPM4 | 1.971099 | 0.0000005 |
| KRT23 | -2.011459 | 0.00004 | B3GAT1 | 1.834909 | 0.0002 |
| LGR6 | -1.843800 | 0.00001 | PRCAT47 | 1.807160 | 0.01 |
| CFD | -1.792887 | 0.00002 | THBS4 | 1.804980 | 0.0001 |
| PTGS1 | -1.750086 | 0.00001 | DLX1 | 1.804387 | 0.0001 |

quality

The statistical programming language R was used to analyse and combine all of the microarray data. Data from Affymetrix and Agilent was initially normalized individually for pre-processing using the preprocessCore package's normalizeQuantiles function (version 1.58.0). (<https://bioconductor.org/packages/release/bioc/html/preprocessCore.html>). With the purpose of exclusion of batch effects (non-biological differences), we used the ComBat function from the R Package Surrogate Variable Analysis (SVA) (version 3.44.0)⁽⁶⁾. Batch effect removal was then evaluated. We showed the result of the meta-analysis in a unit expression matrix.

Assessment of differentially expressed transcripts We used the Limma package (version 3.52.3)⁽⁷⁾ in R language to find differentially expressed mRNAs (DEmRNAs), lncRNAs (DElncRNAs) and miRNAs (DEmiRNAs) between prostate tumor and normal specimens. DEmRNAs, DElncRNAs and DEmiRNAs were appraised with the cut-off criteria of false discovery rate (FDR; adjusted *p* value) < 0.05 and |log₂ fold Change (FC)| > 0.5. Subsequently, we identified DElncRNAs and DEmiRNAs using HUGO gene nomenclature.

Two-Way Clustering of DEGs

Expression levels of significant DEmRNAs, DElncRNAs, and DEmiRNAs were obtained and used in the pheatmap package (version 1.0.12)⁽⁸⁾ in R language to conduct the two-way clustering based on the Euclidean distance.

Gene Ontology (GO) Enrichment

ClusterProfiler R package (version 4.4.4)⁽⁹⁾ was applied to conduct gene ontology (GO) enrichment and investigation of the functions of the significantly up-regulated and down-regulated DEGs. The functional category criteria were established at an adjusted *p*-value < 0.05.

KEGG Pathway Analysis

KEGG pathway analysis of considerable DEGs was performed using the KEGG database⁽¹⁰⁾.

PPI Network Construction

PPI network for DEGs was identified using the STRING database⁽¹¹⁾. Highest level of confidence was utilized to create the interactions parameter (confidence score > 0.9). Protein interactions were visualized using the Cytoscape software v3.9⁽¹²⁾. The top 20 DEGs related to hub genes were lastly detected using the Cytoscape

Table 2. The up- and downregulated DElncRNAs between prostate tumor and normal samples.

| Down-regulated | | | Up-regulated | | |
|----------------|--------------|-------------------------|---------------|-------------|-------------------------|
| DElncRNA | Log FC | Adjusted <i>P</i> value | DElncRNA | Log FC | Adjusted <i>P</i> value |
| UBXN10-AS1 | -1.085041069 | 0.0002 | PCA3 | 2.194085974 | 0.001 |
| FENDRR | -1.001246896 | 0.0002 | LINC00992 | 2.131068688 | 0.00008 |
| MAGI2-AS3 | -0.951283196 | 0.00003 | C1QTNF3-AMACR | 2.129359564 | 0.0001 |
| MAGI2-IT1 | -0.877464251 | 0.0002 | PCAT18 | 1.444563038 | 0.03 |
| BOLA3-AS1 | -0.818242331 | 0.00004 | ERVH48-1 | 1.384998066 | 0.02 |
| ADAMTS9-AS2 | -0.79674974 | 0.00003 | DRAIC | 1.351053821 | 0.006 |
| HCG11 | -0.765278673 | 0.0001 | FOXP4-AS1 | 1.343377023 | 0.0009 |
| TBX5-AS1 | -0.74698408 | 0.00001 | LINC00842 | 1.213140476 | 0.004 |
| RBMS3-AS3 | -0.714422829 | 0.0001 | LINC00920 | 1.030649901 | 0.04 |
| MEG3 | -0.707122105 | 0.0002 | DANCR | 1.026630806 | 0.0005 |
| | | | PRRT3-AS1 | 0.916404009 | 0.03 |
| | | | SNHG19 | 0.900564908 | 0.0001 |
| | | | PCAT7 | 0.827071849 | 0.02 |
| | | | C8orf34-AS1 | 0.824415749 | 0.01 |
| | | | CRNDE | 0.733537617 | 0.01 |
| | | | SNHG9 | 0.711240397 | 0.04 |
| | | | LINC01351 | 0.708756468 | 0.03 |
| | | | ENO1-AS1 | 0.689974397 | 0.01 |
| | | | ZNF793-AS1 | 0.68123815 | 0.009 |
| | | | MCF2L-AS1 | 0.645850215 | 0.007 |
| | | | PRKAG2-AS1 | 0.640111087 | 0.02 |
| | | | PCAT6 | 0.622871409 | 0.02 |
| | | | POU6F2-AS2 | 0.618162182 | 0.03 |
| | | | LINC00862 | 0.596493068 | 0.02 |
| | | | RPARP-AS1 | 0.595574259 | 0.004 |
| | | | LEF1-AS1 | 0.592353189 | 0.02 |
| | | | LINC00665 | 0.538956003 | 0.002 |
| | | | LINC00973 | 0.520799038 | 0.02 |
| | | | LINC01128 | 0.507755709 | 0.005 |

Table 3. The significantly up- and downregulated DEmiRNAs between prostate tumor and normal samples.

| Down-regulated DEmiRNA | | | Up-regulated DEmiRNA | | |
|------------------------|--------------|------------------|----------------------|-------------|------------------|
| DEmiRNA | Log FC | Adjusted P value | DEmiRNA | Log FC | Adjusted P value |
| MIR675 | -1.461212788 | 0.003 | MIR6773 | 1.110887917 | 0.0000363 |
| MIR1908 | -0.809060479 | 0.005 | MIR4683 | 0.903634366 | 0.0003 |
| | | | MIR7110 | 0.875949754 | 0.001 |
| | | | MIR3658 | 0.746514424 | 0.0001 |
| | | | MIR3185 | 0.670389146 | 0.01 |
| | | | MIR6824 | 0.617549387 | 0.02 |
| | | | MIR4647 | 0.599044810 | 0.004 |
| | | | MIR4784 | 0.549181183 | 0.01 |

plugin⁽¹³⁾ of Cytoscape using the betweenness method.

ceRNA Network and Hub Genes

A ceRNA network was constructed through these steps: 1) Searching the miR2Disease database (<http://watson.compbio.iupui.edu:8080/miR2Disease/index.jsp>)⁽¹⁴⁾ utilizing the term "prostate cancer" for the prostate cancer (PC)-related miRNAs. 2) measuring the interactions between lncRNAs and miRNAs based on the PC-related miRNAs using miRcode (<http://www.mircode.org/>); 2) Application of miRDB (<http://www.mirdb.org/>)⁽¹⁵⁾, miRTarBase (<https://mirtarbase.cuhk.edu.cn/>)⁽¹⁶⁾, TargetScan (<http://www.targetscan.org/>)⁽¹⁷⁾ and miRWalk (<http://129.206.7.150/>)⁽¹⁸⁾ for predicting miRNAs-targeted mRNAs; 3) Discovery of the intersections of the DElncRNAs and DEmRNAs, and formation of lncRNA/mRNA/miRNA ceRNA network using Cytoscape v3.9 and 4) predicting hub genes using cytohubba plugin based on degree approach.

Confirmation of hub genes via expression values

Expression value of hub genes was evaluated using the ualcan database⁽¹⁹⁾.

Survival analysis

Survival package (version 3.5.0) (<https://CRAN.R-project.org/package=survival>) in R was utilized to find survival curves. The clinical data for patients with prostate cancer was obtained from TCGA (PRAD-TCGA). Univariate survival analysis was performed using Kaplan-Meier curves. Statistics were considered significant for P -value < 0.05 . The start time to the end time in this analysis is from 0 to 5000 days.

RESULTS

Microarray Data Processing

Figure 1 depicts the boxplots of raw data, normalized data after batch effect removal and quantile normalization. These plots show the reliability of the quality of the expression data. Moreover, the boxplot of the pre-processed data had good normalization. **Figure 2** shows the Euclidean distances between the samples after batch effect removal. In the PCA plot (**Figure 3**), 101 specimens are shown in the 2D plane traversed by their first two principal components (PC1 and PC2) According to

this plot, the samples had a good dispersion following the removal of batch effect.

DEGs Analysis

Based on the microarray data analysis between prostate tumor and normal samples by Limma, we analyzed differentially expressed mRNA, lncRNA and miRNAs and obtained 1312 DE mRNAs, including 778 down-regulated DE mRNAs (such as CXCL13 and BMP5) and 584 upregulated DE mRNAs (such as OR51E2 and LUZP2), 39 DE lncRNAs, including 10 downregulated DE lncRNAs (such as UBXL10-AS1 and FENDRR) and 29 upregulated DE lncRNAs (such as PCA3 and LINC00992) and 10 DE miRNAs, including 2 down-regulated DE miRNAs (such as MIR675 and MIR1908) and 8 upregulated DE miRNAs (such as MIR6773 and MIR4683). The most significantly upregulated and downregulated DE mRNAs, DE lncRNAs, and DE miRNAs are shown in **Tables 1-3**, respectively.

Volcano plot was depicted with the EnhancedVolcano package (version 1.14.0)⁽²⁰⁾ in R to compare the variation in miRNA, lncRNA, and mRNA expression between prostate tumor and normal samples (**Figure 4**). Moreover, the two-way clustering showed 20 clearly distinct DE mRNA expression patterns between prostate tumor and normal samples (**Figure 5a**). The expression of DE lncRNAs and DE miRNAs is demonstrated in two heatmaps (**Figure 5b**).

GO Enrichment Analysis of DEGs

The substantially DEGs were enriched in 497 GO terms. ClusterProfiler package was used for analysis. For performing this analysis, the all genes listed in the database in clusterProfiler package have been used as background. In GO functional enrichment analysis, 497 GO entries fulfil Adjusted P value < 0.05 , the majority of which are biological processes, followed by cellular component and molecular function. The first 30 entries are collagen-containing extracellular matrix (CC), extracellular matrix structural constituent (MF), extracellular matrix organization (BP), extracellular structure organization (BP), cell-cell junction (CC), basement membrane (CC), cell junction assembly (BP), cell-substrate adhesion (BP), collagen trimer (CC), sarcolemma (CC), muscle contraction (BP), muscle system process

Table 4. Down-regulated and Up-regulated Pathways

| Down-regulated Pathway | | Up-regulated Pathway | |
|-------------------------------------|-------------|----------------------|------------|
| Pathway | P value | Pathway | P value |
| Focal adhesion | 0.007574712 | Purine metabolism | 0.04602828 |
| Protein digestion and absorption | 0.014154194 | | |
| Vascular smooth muscle contraction | 0.023808509 | | |
| ECM-receptor interaction | 0.031880880 | | |
| Complement and coagulation cascades | 0.049110016 | | |

Table 5. The MiRcode database demonstrated interactions between 13 DElncRNAs and 13 DEmiRNAs.

| lncRNA | miRNA |
|---|-------------|
| PCA3, ERVH48-1, ADAMTS9-AS2, RBMS3-AS3, MEG3 | miR-96 |
| PCA3, ERVH48-1, ADAMTS9-AS2, BOLA3-AS1, RBMS3-AS3, MEG3 | miR-182 |
| PCA3, CRNDE, ADAMTS9-AS2, MEG3 | miR-221 |
| PCA3, CRNDE, ADAMTS9-AS2, MEG3 | miR-222 |
| MCF2L-AS1, CRNDE, ADAMTS9-AS2, HCG11, MEG3 | miR-205 |
| ENO1-AS1, CRNDE, ERVH48-1, MAGI2-AS3, ADAMTS9-AS2, MEG3 | miR-145 |
| CRNDE, SNHG9, MAGI2-AS3, ADAMTS9-AS2, HCG11, MEG3 | miR-31 |
| CRNDE, ERVH48-1, MAGI2-AS3, ADAMTS9-AS2, HCG11, MEG3 | miR-181b |
| CRNDE, ADAMTS9-AS2 | miR-183 |
| ERVH48-1, SNHG9, ADAMTS9-AS2, BOLA3-AS1, MEG3 | miR-184 |
| POU6F2-AS2, ADAMTS9-AS2, | miR-375 |
| POU6F2-AS2, MEG3 | miR-125b-5p |
| MAGI2-AS3, MEG3 | miR-16 |

Table 6. miRWalk, miRDB and TargetScan databases revealed interactions between 10 DEmiRNAs and 24 DEMRNAs.

| miRNA | mRNA |
|-------------|---|
| miR-96 | TP53INP1, NIPA1 |
| miR-182 | FOXF2 |
| miR-221 | TRPS1, KIT |
| miR-222 | STOX2, TRPS1 |
| miR-205 | LRRK2 |
| miR-145 | ADD3, TGFB2, MYO6 |
| miR-31 | SPRED1 |
| miR-181b | KLHL15, PLPP3, PLAG1 |
| miR-16 | RAB9B, GALNT7, PSAT1, TGFB3, PDLIM5, SLC9A6 |
| miR-125b-5p | MFSD9, STOX2, HK2 |

(BP), urogenital system development (BP), morphogenesis of a branching structure (BP), I band (CC), endoplasmic reticulum lumen (CC), extracellular matrix structural constituent conferring tensile strength (MF), contractile fiber (CC), regulation of cell-substrate adhesion (BP), Z disc (CC), mesenchyme development (BP), mesenchymal cell differentiation (BP), respiratory tube development (BP), myofibril (CC), membrane raft (CC), membrane microdomain (CC), gland morphogenesis (BP), renal system development (BP), glycosaminoglycan binding (MF) and sarcomere (CC). **Figure 6** shows the barplots of top 10 enriched functions.

Pathway Analysis

Using Pathview (version 1.36.1)⁽²¹⁾ and gage (version 2.46.1)⁽²²⁾ packages in R, KEGG pathway analyses of 177 down-regulated and 177 up-regulated DEGs were performed to identify the potential functional genes (**Table 4 and Figure 11**). **Figure 10** shows the schematic visualization of 3 pathways (1 up-regulated and 2 down-regulated pathways).

PPI network construction and selection of hub genes
In order to find the hub genes, a PPI network of DEGs (supplementary file) with 411 nodes and 555 edges that was acquired from STRING was loaded into the Cytohubba plugin of Cytoscape 3.9. The 20 hub genes with the highest betweenness of connectivity were EGF,

PRKCA, FLNA, CAV1, RGS9, RGS2, CD3EAP, RRM2, ITGA1, PPP1R12B, SDC2, MLC1, PRKG1, BIRC5, P4HB, FGFR2, POLR2H, VCL, PIK3R1 and RGS17.

LncRNAs can act as an endogenous "sponge" to regulate the expression of mRNA by adsorbing miRNA, according to the ceRNA theory⁽²³⁾. The lncRNA-miRNA-mRNA ceRNA network was built using upregulated or down-regulated miRNAs, as well as lncRNAs or mRNAs⁽²⁴⁾. DElncRNAs and DEmiRNAs networks did not interact in our research. We utilized the miR2Disease database as a result. In miR2Disease, we chose miRNAs that changed in prostate tumor tissues compared to adjacent normal tissue samples, both up- and down-regulating. We discovered 14 PC-related miRNAs using the miR2 Disease database. The relationship between lncRNAs and miRNAs was then evaluated using miRcode. This step showed that 13 of 14 PC-specific miRNAs may target to the 13 of 39 DElncRNAs (**Table 5**). Then we used miRDB, miRTarBase, TargetScan and miRWalk to predict targeted mRNAs by these 13 miRNAs to discover the relationship between miRNAs and mRNAs. We found that 10 miRNAs might target 24 out of the 1312 mRNAs (**Table 6**). If miRNA-targeted mRNAs were not found in DEMRNAs, they were eliminated. Using this information (**Table 5 and 6**), we used Cytoscape 3.9 to construct the lncRNA-miRNA-mRNA ceRNA network. Once the targeted DEMRNAs and DElncRNAs' expression patterns were reversed, DElncRNAs, targeted DEMRNAs, and the interacting miRNAs were all eliminated from the ceRNA network. A total of 8 lncRNAs, 4 mRNAs, and 3 miRNAs were included in the ceRNA network (**Figure 13**). At last, we computed nodes degrees and displayed the top 7 nodes with the highest degree in the network using cytohubba app (**Figure 14**). We found ENO1-AS1, hsa-miR-182, hsa-miR-125b-5p, hsa-miR-145, MEG3, FOXF2 and MYO6 as 7 hub genes in ceRNA network.

Confirmation of hub genes via expression value

The expression value of hub genes was evaluated using the ualcan database. As a result, all hub genes in PPI network and MIR182 in ceRNA network indicated good statistical significance (**Figure 16 and Table 7**).
Survival analysis

For survival analysis, we downloaded and analyzed transcriptome profiling of prostate cancer samples (TCGA-PRAD) using TCGAbiolinks (version 2.24.3)⁽²⁵⁾ and edgeR (version 3.38.4)⁽²⁶⁾ packages. Survival was analyzed based on Kaplan-Meier curves using surviv-

Table 7. Statistical significance of hub genes based on sample types in prostate cancer.

| Hub genes | Statistical significance of expression value |
|-----------|--|
| POLR2H | <1E-12 |
| CAV1 | 2.23E-08 |
| ITGA1 | 4.22E-05 |
| PIK3R1 | 3.79E-10 |
| RGS9 | 5.79E-05 |
| SDC2 | 1.25E-04 |
| P4HB | <1E-12 |
| PPP1R12B | 1.13E-06 |
| RRM2 | 2.32E-07 |
| PRKCA | 2.07E-06 |
| VCL | 7.55E-07 |
| BIRC5 | 7.23E-11 |
| CD3EAP | 4.68E-08 |
| PRKG1 | 4.22E-06 |
| FLNA | 3.27E-07 |
| MLC1 | 1.03E-04 |
| RGS2 | 3.40E-04 |
| EGF | 4.02E-13 |
| RGS17 | 9.88E-05 |
| FGFR2 | <1E-12 |
| MIR182 | <1E-12 |



Figure 1. Boxplots after combining datasets. **A)** First box plot shows the combination of datasets **B)** The second boxplot shows the merged datasets after removing the batch effect removal.

al package in R. We performed survival analysis based on hub genes in PPI and ceRNA networks. The difference was statistically significant with log-rank $P < 0.05$. RRM2 and MYO6 showed a strong correlation with a reduced overall survival time in individuals with pros-

tate cancer (**Figure 17**).

DISCUSSION

ceRNA networks have been found to participate in the pathoetiology of several cancers, including prostate cancer. Unraveling the interactions between constitu-

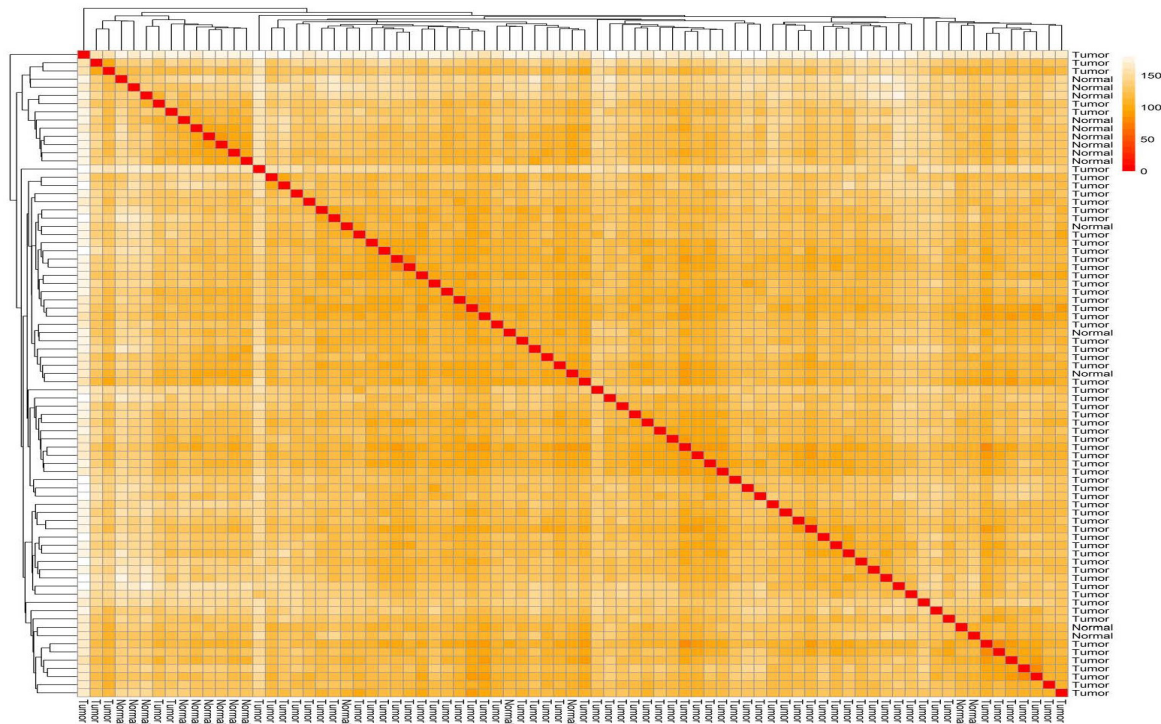


Figure 2. The Euclidean distances between samples. Based on the Euclidean distance, hierarchical clustering between the samples has been established; Legend shows the distance value between samples.

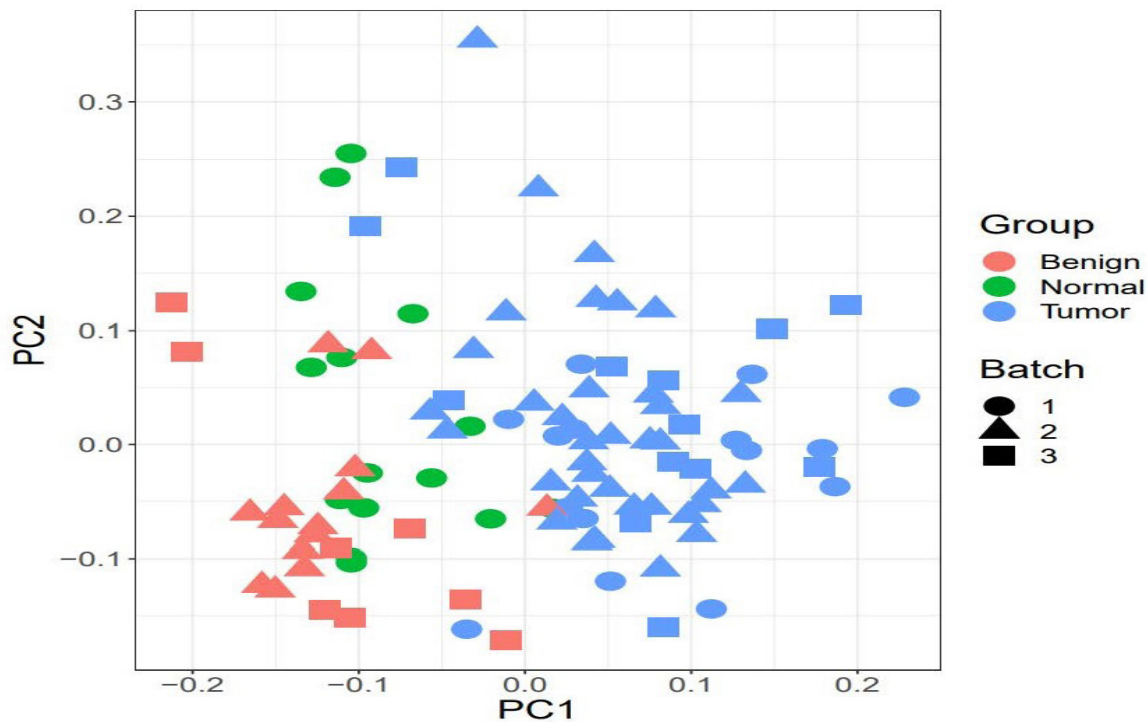


Figure 3. PCA plot. The Batch implies that the data includes three platforms. Also, healthy benign and tumor samples were divided into three groups.

ents of these networks can facilitate the identification of the most relevant cancer-specific pathogenic events. The current study aimed at the construction of ceRNA network in prostate cancer.

We obtained 1312 DEmRNAs, including 778 down-regulated DEmRNAs (such as CXCL13 and BMP5) and 584 up-regulated DEmRNAs (such as OR51E2 and LUZP2). BMP5 has been previously shown to be an im-

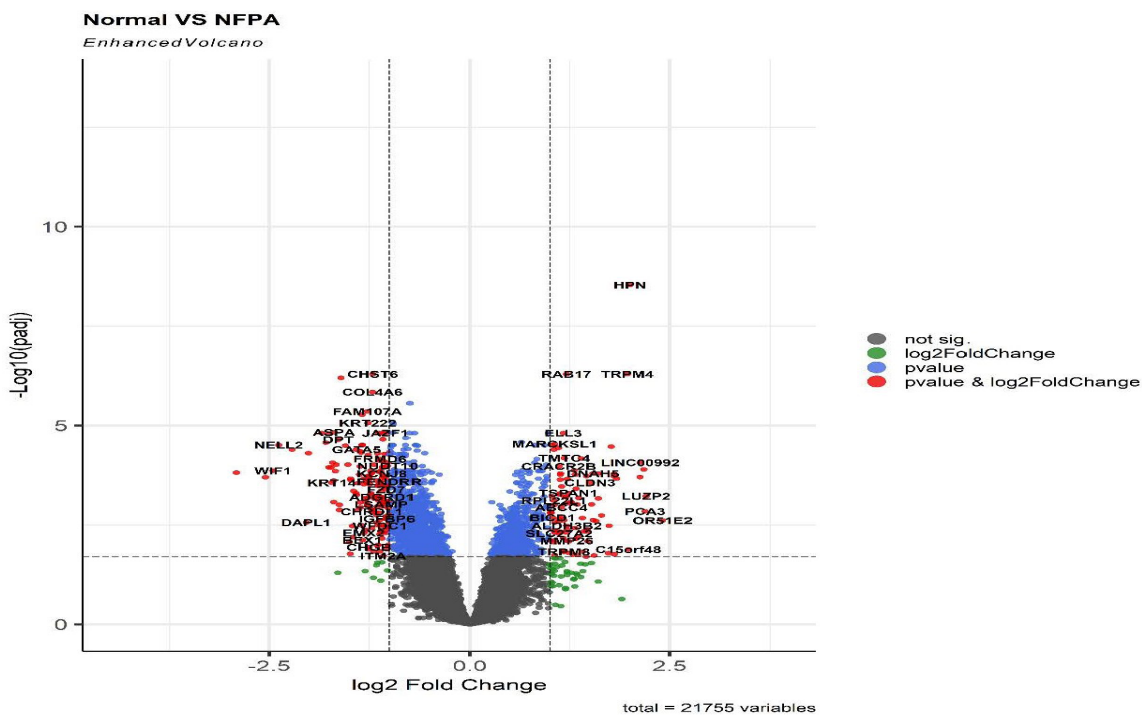


Figure 4. The volcano plot of differentially expressed genes (DEGs); horizontal axis, log2(FC); vertical axis, -log10(adjusted P value).

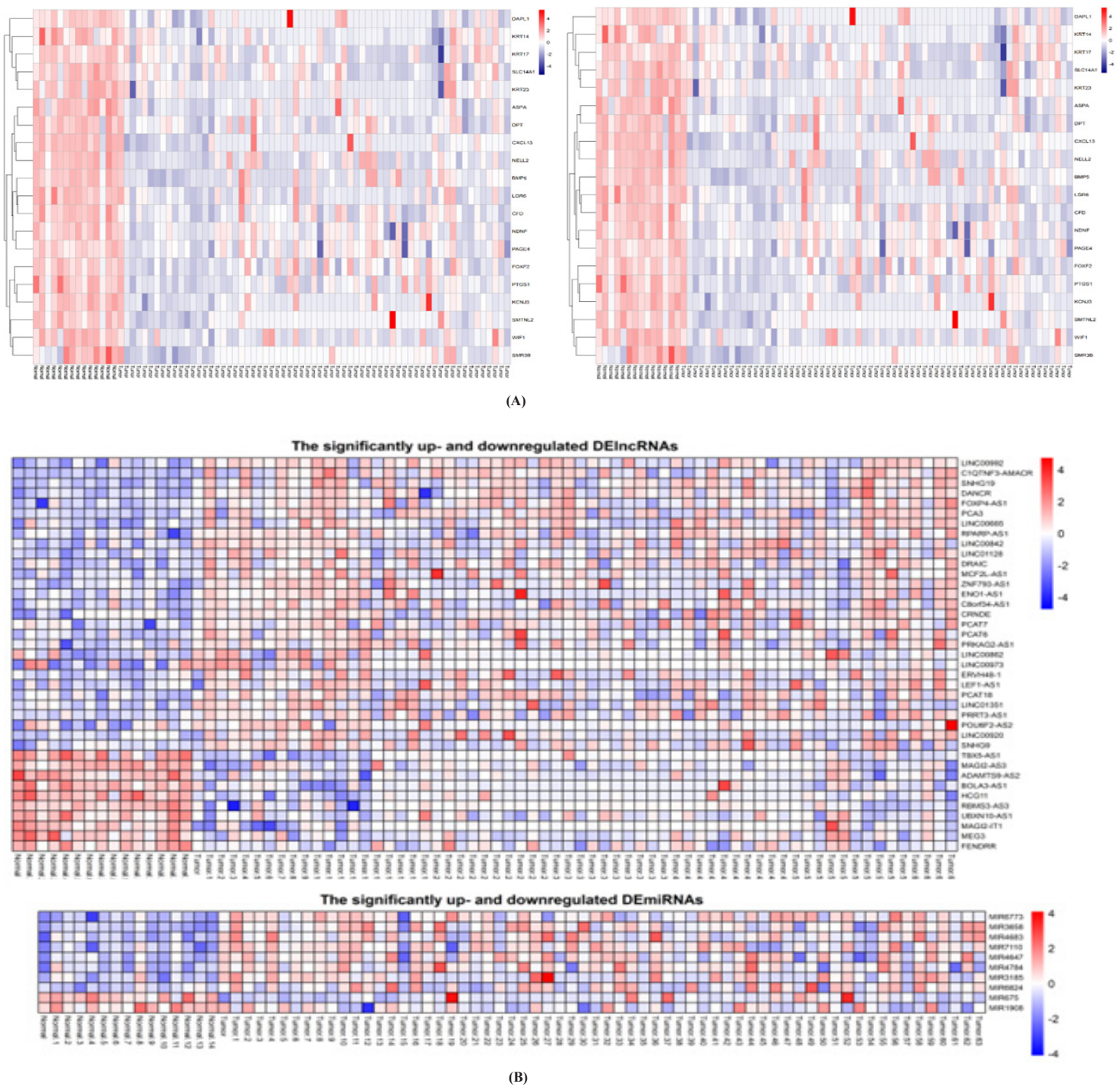


Figure 5. A. The two-way clustering of DEMRNAs between prostate tumor samples and normal samples; horizontal axis, the samples; vertical axis, DEMRNAs. **B.** Two heatmaps depicting expression of DElncRNAs and DEMiRNAs.

portant regulator of basal prostate stem cell homeostasis being involved in the initiation of prostate cancer⁽²⁷⁾. In addition, CXCL13 is an androgen-responsive gene participating in the androgen-regulated migration and invasion of prostate cancer cells⁽²⁸⁾. On the other hand, OR51E2 has been shown to inhibit proliferation and induce prostate cancer cell death⁽²⁹⁾. LUZP2 has been previously reported to be over-expressed in hormone-naive

prostate cancer but its expression has been decreased in the course of evolution of hormone-naive prostate cancer to castration-resistant ones⁽³⁰⁾. Moreover, we found 39 DElncRNAs, including 10 down-regulated DElncRNAs (such as UBXN10-AS1 and FENDRR) and 29 up-regulated DElncRNAs (such as PCA3 and LINC00992) and 10 DEMiRNAs, including 2 down-regulated DEMiRNAs (such as MIR675

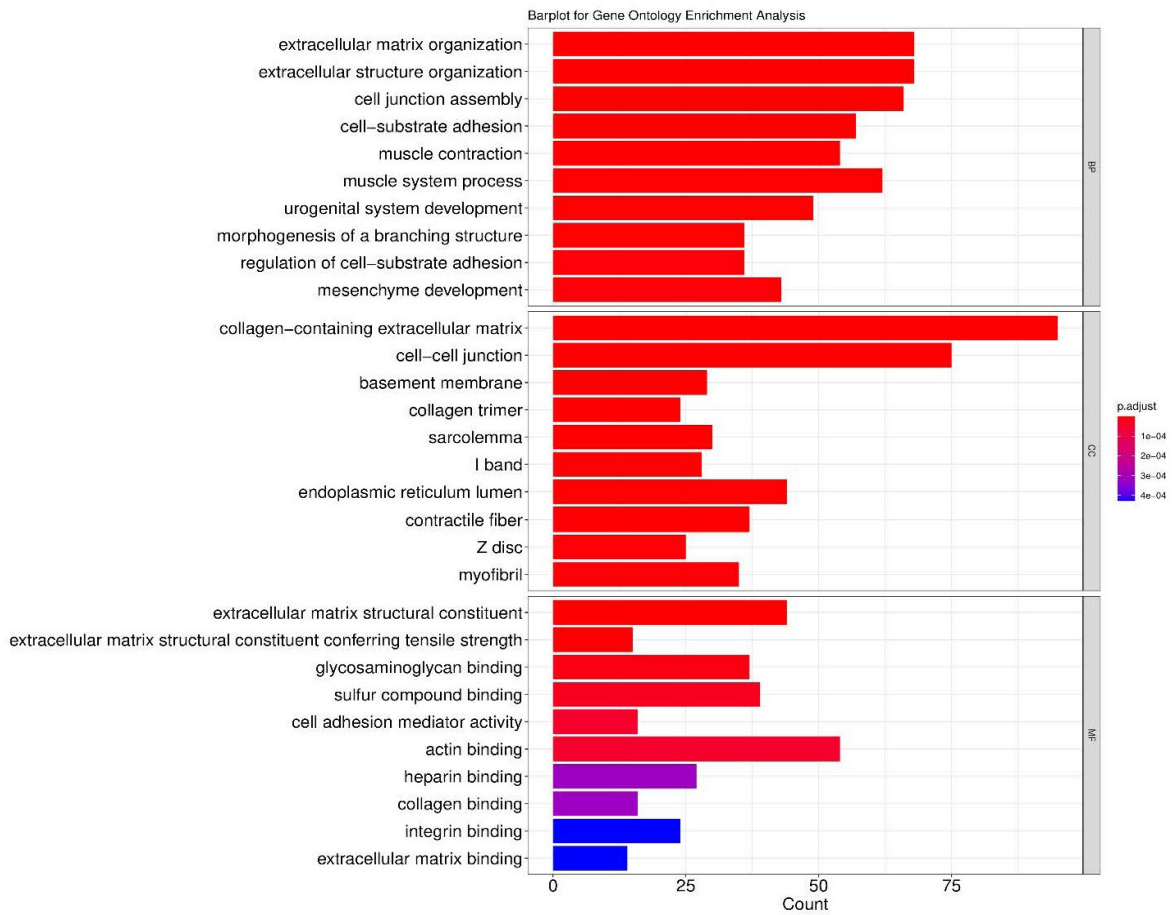


Figure 6. The barplots of top 10 enriched functions. BP (biological process), CC (cellular component) and MF (molecular function). X axis displays the count of geneset; Y axis displays the geneset function; Bar color signifies the adjusted P.value, ranging from red (most significant) to blue (least significant).

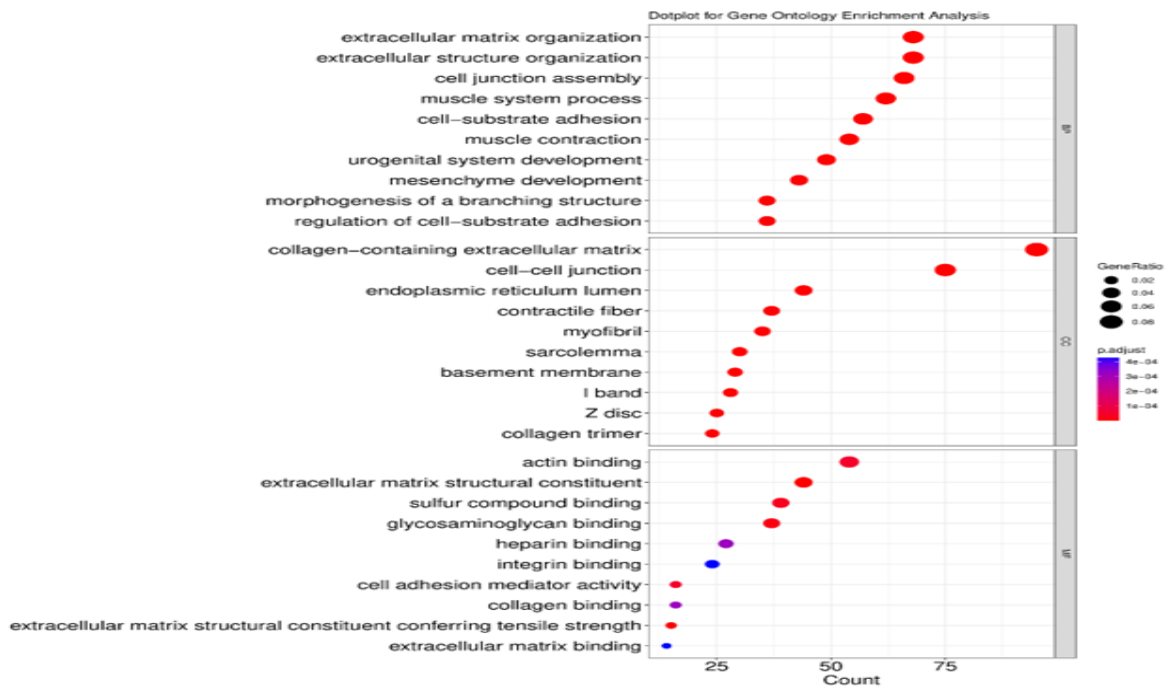


Figure 7. The dotplots of top 10 enriched functions. X axis displays the count of geneset; Y axis displays the geneset function; Dot color represents the adjusted P.value, ranging from dark blue (most significant) to red (least significant). Dot size represents the GeneRatio and The larger the size of the dot, the higher the value of the gene ratio.

Gene-Concept Network for GO Enrichment Analysis

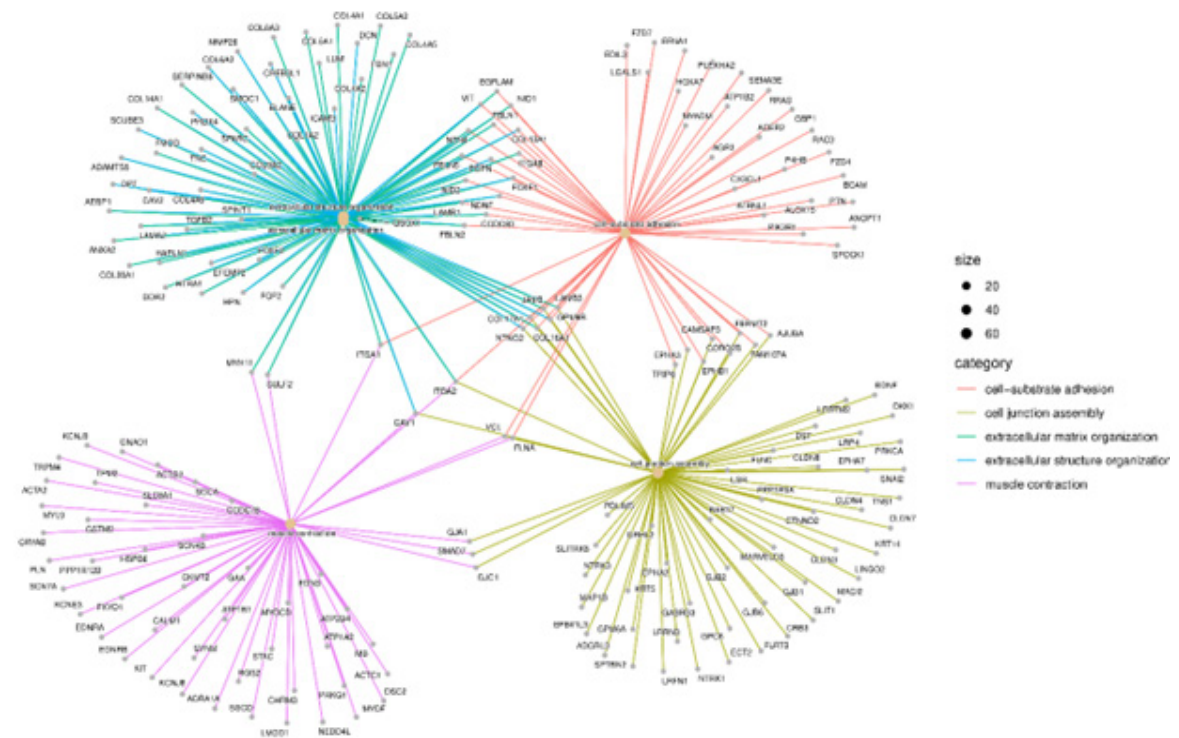


Figure 9. Network plot of top 5 GO terms. GO terms are linked with genes. There are more genes for a specific GO term if the dot relating to it is bigger.

In figure 10, the UpSet plot visualized the intersection between top 10 GO terms. It highlights the gene overlap between several gene sets.

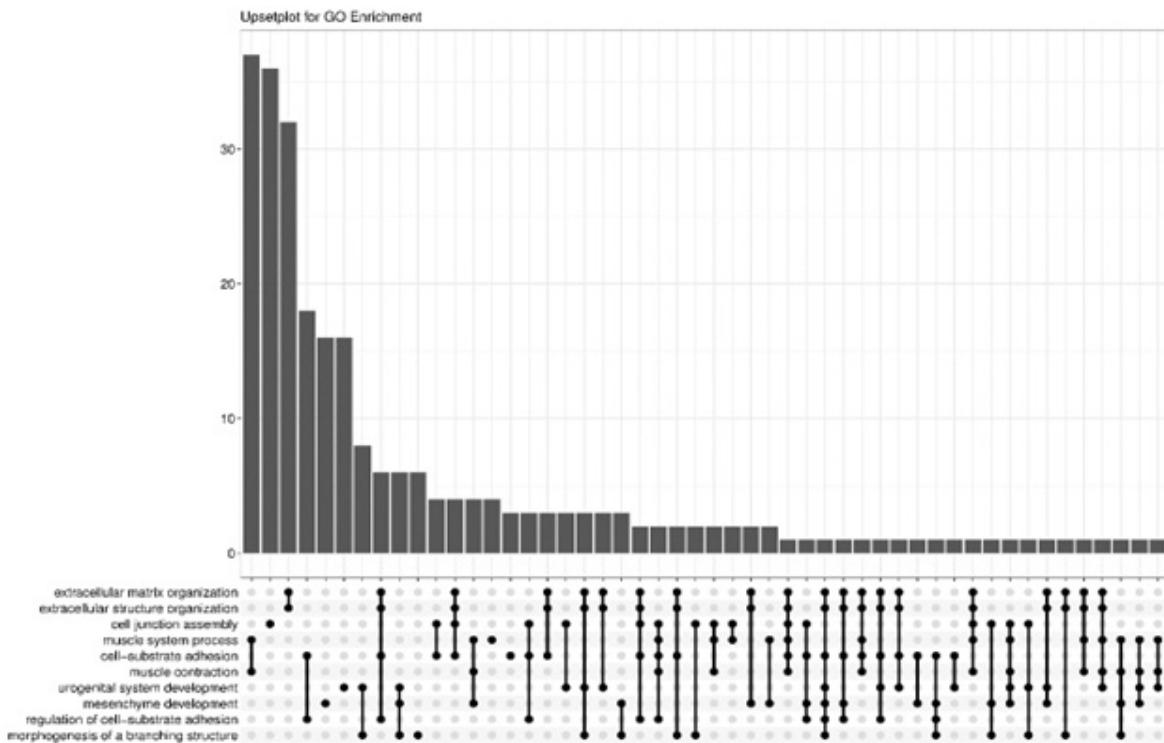
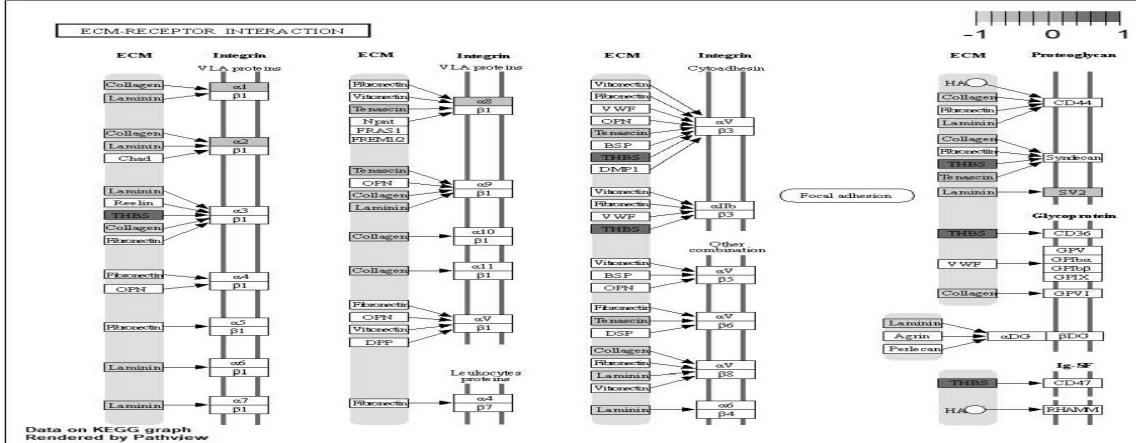
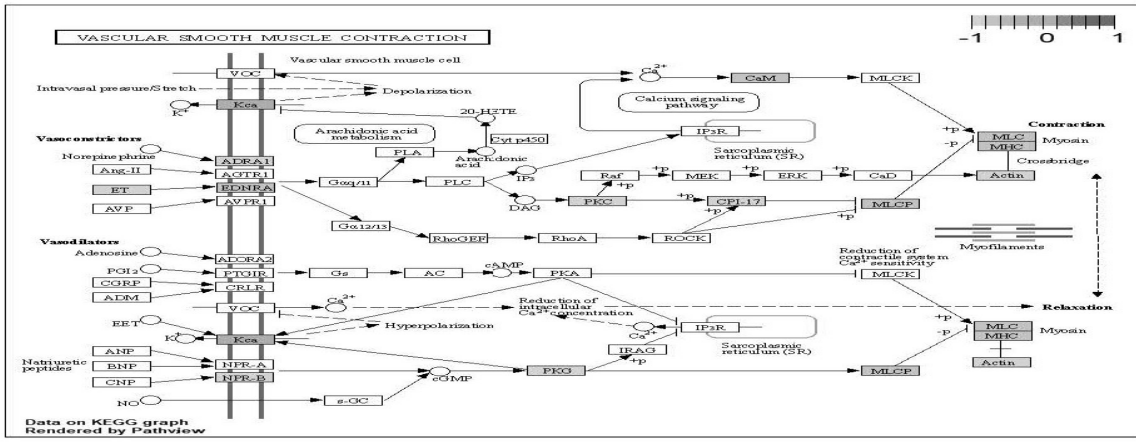
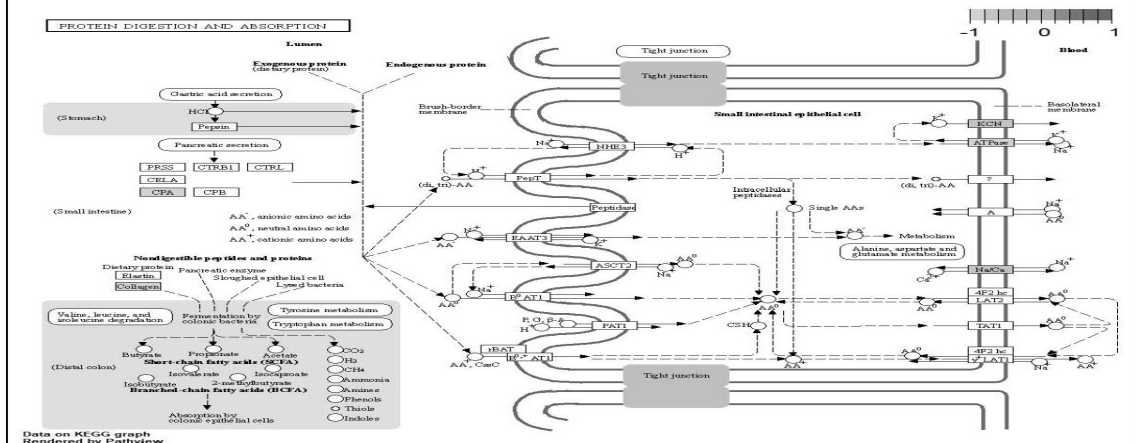
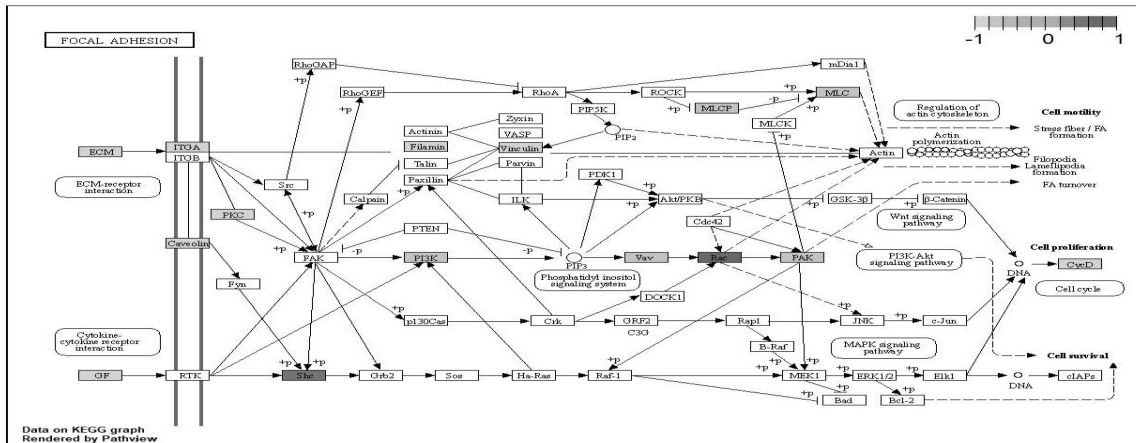


Figure 10. UpsetPlot of 10 GO terms.



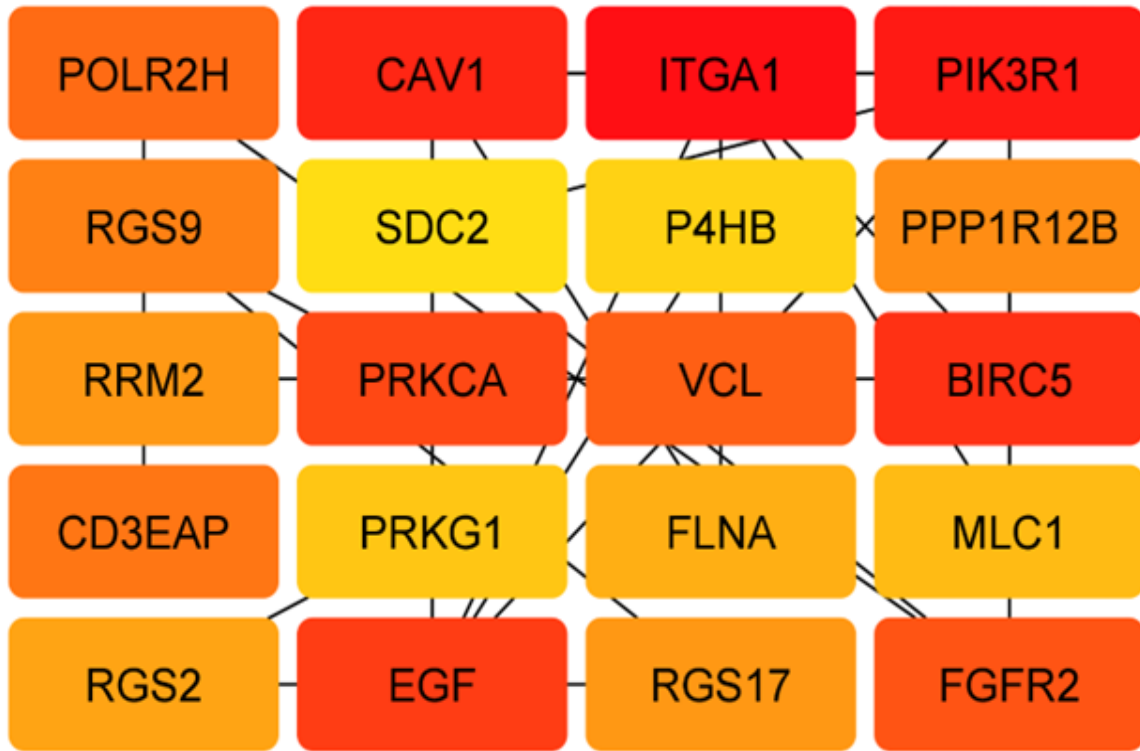


Figure 12. 20 hub genes with the highest betweenness of connectivity.

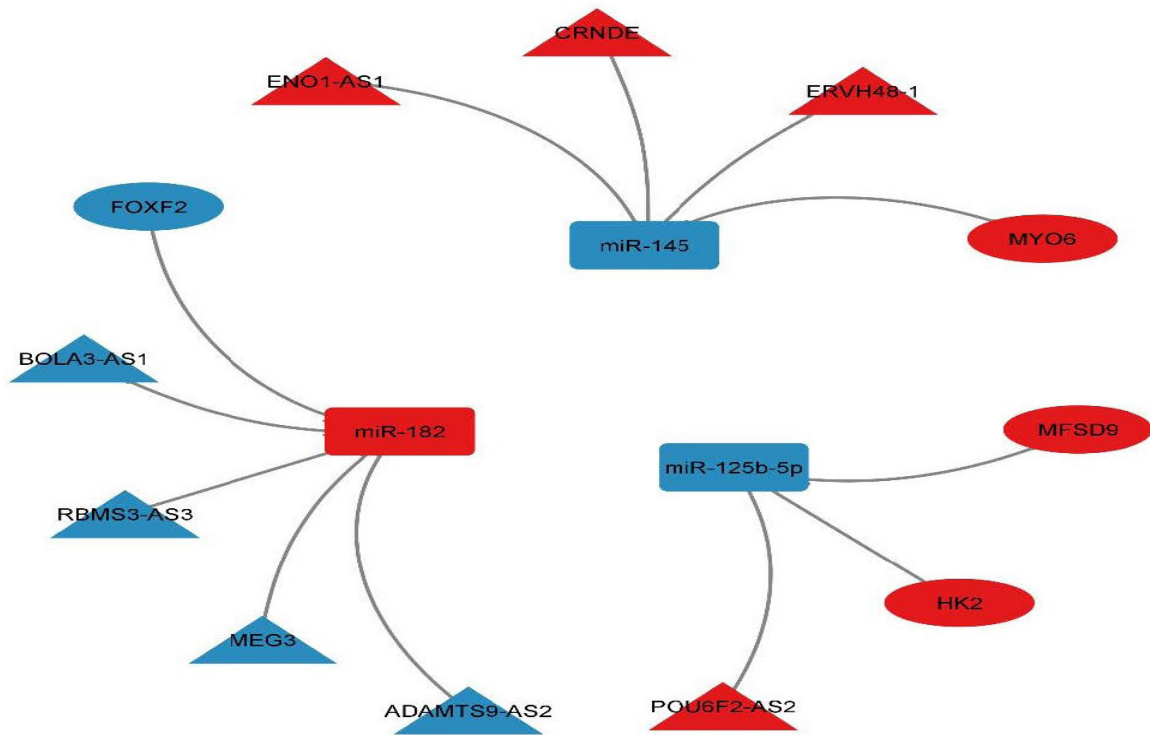


Figure 13. CeRNA network in prostate cancer. Red nodes mean a strong expression level, while blue nodes signify a low level of expression. Ellipses show protein-coding genes; rectangles show miRNAs; Triangles show lncRNAs; gray edges designate lncRNA-miRNA-mRNA interaction.

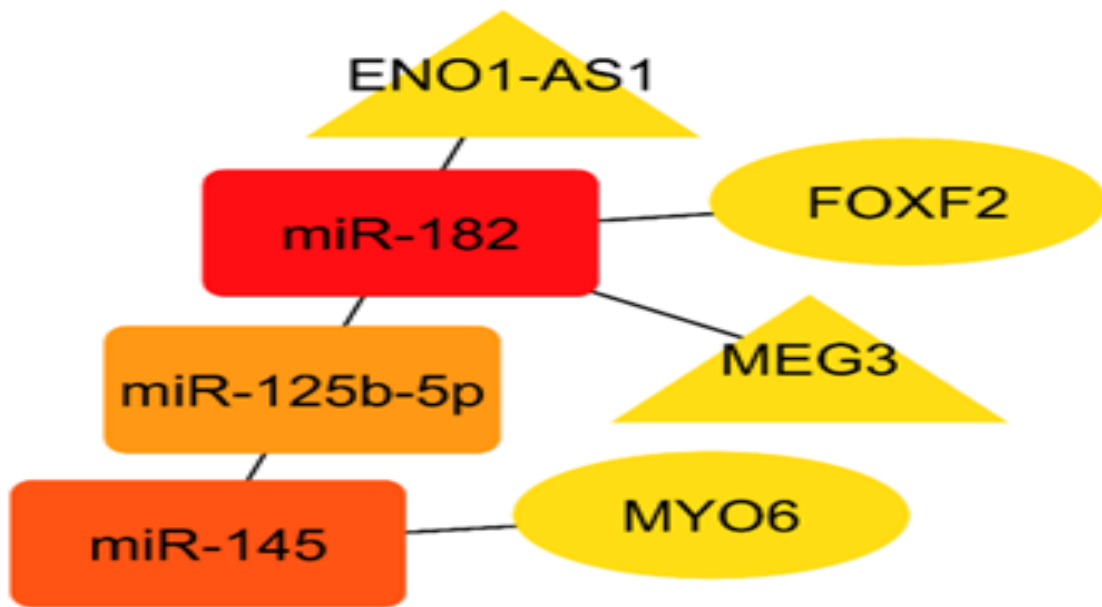


Figure 14. Top 7 genes with highest degree in ceRNA network.

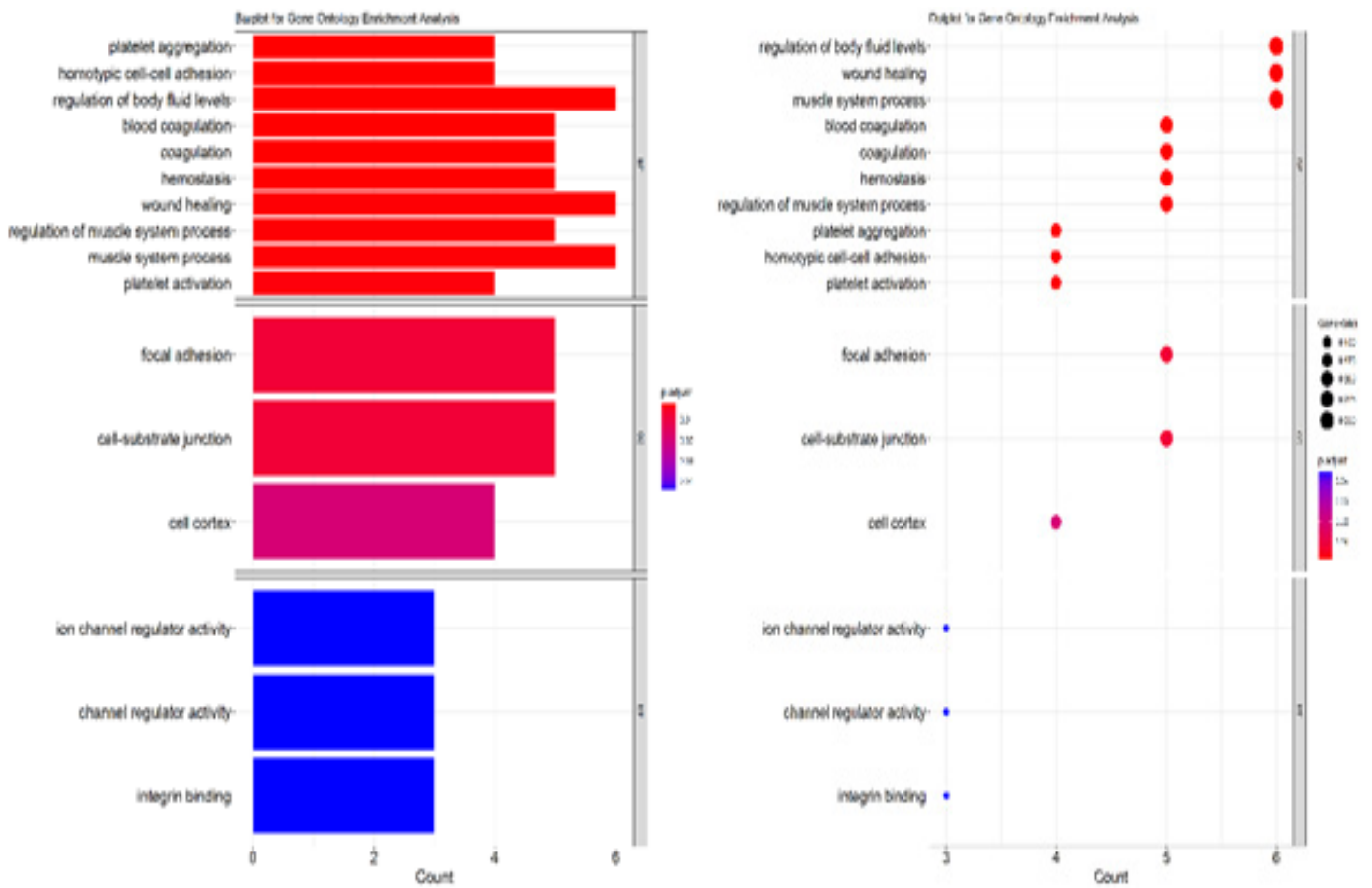


Figure 15. Gene ontology enrichment analysis of the target genes in the networks. Barplot and dotplot indicate top functional terms related to hub genes.

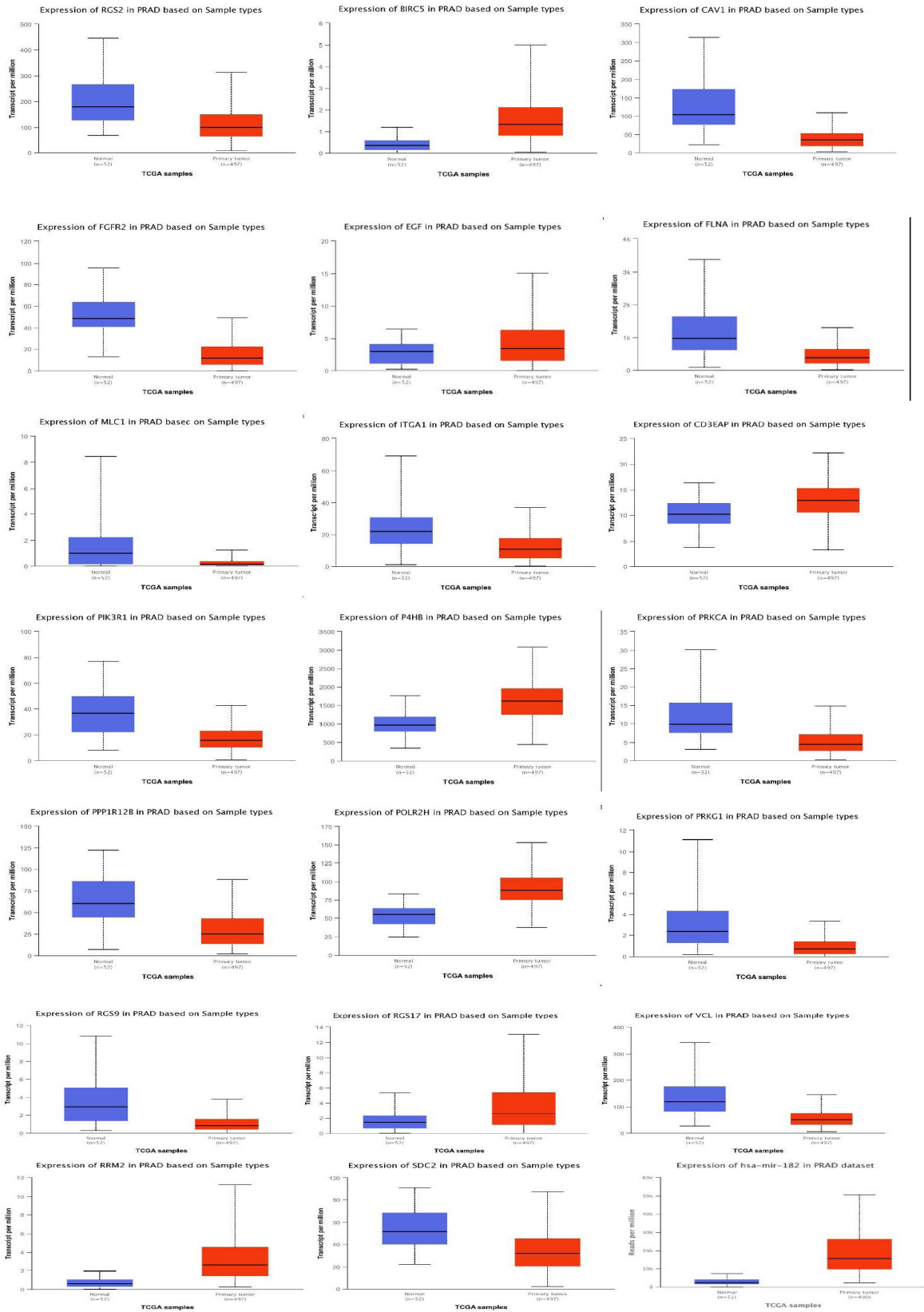


Figure 16. Box plots of gene expression of hub genes in prostate tumor and healthy samples based on TCGA. Red and green boxes show gene expression of hub genes in prostate tumor and healthy samples, respectively.

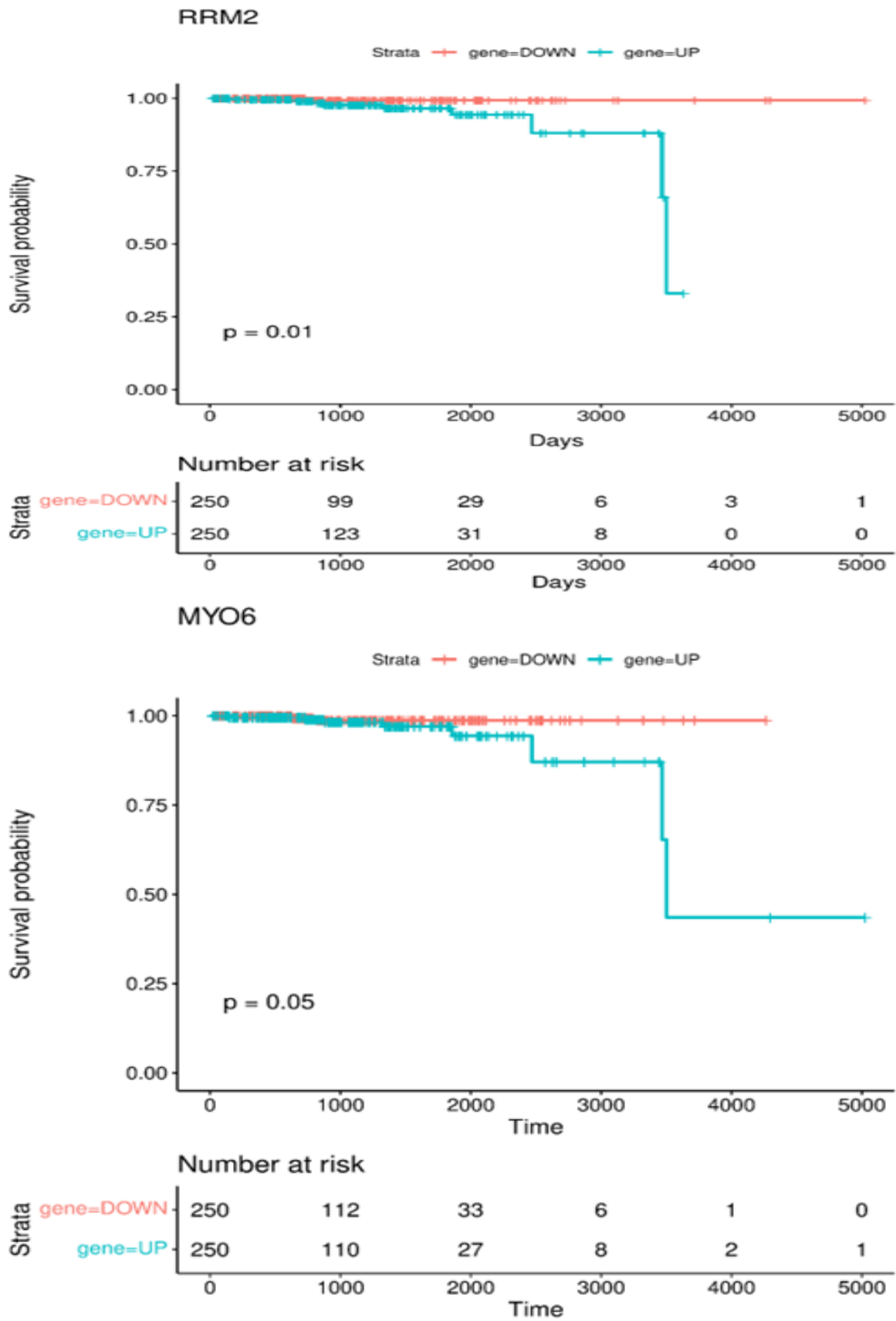


Figure 17. RRM2 and MYO6 Kaplan-Meier survival curves is related to patients with prostate cancer's overall survival.

metabolism by purinosome is a multi-enzyme complex located around mitochondria and microtubules. Purinosome has been emphasized for its therapeutic potential in cancers (Yin et al., 2018; *Frontiers Immunology*). These analyses point towards a novel identified ceRNA network of metastatic potential in prostate cancer.

Thus, several important cancer-related pathways linked to each other are modulated by the identified ceRNA networks in the current study.

We also evaluated the significance of these RNAs in the determination of survival of patients with prostate cancer. Among the dysregulated genes, RRM2 showed a strong correlation with a reduced overall survival time in individuals with prostate cancer. RRM2 codes one of two subunits of ribonucleotide reductase. This enzyme facilitates conversion of ribonucleotides to deoxyribonucleotides. Expression of the encoded protein by this gene is controlled during the progression of cell-cycle. This protein is up-regulated in several cancers and is involved in the gemcitabine metabolism. Thus, RRM2 has been suggested as a marker for chemotherapy response and prognosis. It's up-regulation can facilitate DNA damage repair and affect activity of signaling cascades⁽³²⁾. Future studies are needed to find the underlying mechanism of participation of this gene in the course of prostate cancer.

This study provides novel candidates for design of specific treatment modalities for prostate cancer and broadens the current insight about the role of non-coding RNAs in the pathogenesis of prostate cancer.

AVAILABILITY OF DATA AND MATERIALS

The analyzed data sets generated during the study are available from the corresponding author on reasonable request.

COMPETING INTEREST

The authors declare they have no conflict of interest

APPENDIX

<https://journals.sbm.ac.ir/urolj/index.php/uj/libraryFiles/downloadPublic/59>

REFERENCES

- Zhang X, Wang W, Zhu W, Dong J, Cheng Y, Yin Z, et al. Mechanisms and Functions of Long Non-Coding RNAs at Multiple Regulatory Levels. *International journal of molecular sciences*. 2019;20(22).
- Thomson DW, Dinger ME. Endogenous microRNA sponges: evidence and controversy. *Nature Reviews Genetics*. 2016;17(5):272-83.
- Sung H, Ferlay J, Siegel RL, Laversanne M, Soerjomataram I, Jemal A, et al. Global Cancer Statistics 2020: GLOBOCAN Estimates of Incidence and Mortality Worldwide for 36 Cancers in 185 Countries. *CA: a cancer journal for clinicians*. 2021;71(3):209-49.
- Li F, Li H, Hou Y. Identification and analysis of survival-associated ceRNA triplets in prostate adenocarcinoma. *Oncology letters*. 2019;18(4):4040-7.
- Guo Z, Han L, Fu Y, Wu Z, Ma Y, Li Y, et al. Systematic Evaluation of the Diagnostic and Prognostic Significance of Competitive Endogenous RNA Networks in Prostate Cancer. *Frontiers in genetics*. 2020;11:785.
- Leek JT, Johnson WE, Parker HS, Jaffe AE, Storey JD. The sva package for removing batch effects and other unwanted variation in high-throughput experiments. *Bioinformatics*. 2012;28(6):882-3.
- Ritchie ME, Phipson B, Wu D, Hu Y, Law CW, Shi W, et al. limma powers differential expression analyses for RNA-sequencing and microarray studies. *Nucleic Acids Res*. 2015;43(7):e47.
- Guo K, Jin F. NFAT5 promotes proliferation and migration of lung adenocarcinoma cells in part through regulating AQP5 expression. *Biochemical and Biophysical Research Communications*. 2015;465(3):644-9.
- Wu T, Hu E, Xu S, Chen M, Guo P, Dai Z, et al. clusterProfiler 4.0: A universal enrichment tool for interpreting omics data. *Innovation (Camb)*. 2021;2(3):100141.
- Kanehisa M, Goto S. KEGG: kyoto encyclopedia of genes and genomes. *Nucleic Acids Res*. 2000;28(1):27-30.
- Szklarczyk D, Franceschini A, Wyder S, Forslund K, Heller D, Huerta-Cepas J, et al. STRING v10: protein-protein interaction networks, integrated over the tree of life. *Nucleic Acids Res*. 2015;43(Database issue):D447-52.
- Shannon P, Markiel A, Ozier O, Baliga NS, Wang JT, Ramage D, et al. Cytoscape: a software environment for integrated models of biomolecular interaction networks. *Genome Res*. 2003;13(11):2498-504.
- Chin C-H, Chen S-H, Wu H-H, Ho C-W, Ko M-T, Lin C-Y. cytoHubba: identifying hub objects and sub-networks from complex interactome. *BMC Systems Biology*. 2014;8(4):S11.
- Jiang Q, Wang Y, Hao Y, Juan L, Teng M, Zhang X, et al. miR2Disease: a manually curated database for microRNA deregulation in human disease. *Nucleic Acids Res*. 2009;37(Database issue):D98-104.
- Chen Y, Wang X. miRDB: an online database for prediction of functional microRNA targets. *Nucleic Acids Res*. 2020;48(D1):D127-d31.
- Huang HY, Lin YC, Li J, Huang KY, Shrestha S, Hong HC, et al. miRTarBase 2020: updates to the experimentally validated microRNA-target interaction database. *Nucleic Acids Res*. 2020;48(D1):D148-d54.
- Agarwal V, Bell GW, Nam JW, Bartel DP. Predicting effective microRNA target sites in mammalian mRNAs. *Elife*. 2015;4.
- Sticht C, De La Torre C, Parveen A, Gretz N. miRWalk: An online resource for prediction of microRNA binding sites. *PLoS One*. 2018;13(10):e0206239.
- Chandrashekar DS, Bashel B, Balasubramanya SAH, Creighton CJ, Ponce-Rodriguez I, Chakvarathi B, et al. UALCAN: A Portal for Facilitating Tumor Subgroup Gene Expression and Survival Analyses. *Neoplasia*. 2017;19(8):649-58.
- Wu J, Liu T, Rios Z, Mei Q, Lin X, Cao S.

- Heat shock proteins and cancer. *Trends in pharmacological sciences*. 2017;38(3):226-56.
21. Luo W, Brouwer C. Pathview: an R/Bioconductor package for pathway-based data integration and visualization. *Bioinformatics*. 2013;29(14):1830-1.
 22. Luo W, Friedman MS, Shedden K, Hankenson KD, Woolf PJ. GAGE: generally applicable gene set enrichment for pathway analysis. *BMC Bioinformatics*. 2009;10(1):161.
 23. Guo LL, Song CH, Wang P, Dai LP, Zhang JY, Wang KJ. Competing endogenous RNA networks and gastric cancer. *World J Gastroenterol*. 2015;21(41):11680-7.
 24. Xu Y, Chen J, Yang Z, Xu L. Identification of RNA Expression Profiles in Thyroid Cancer to Construct a Competing Endogenous RNA (ceRNA) Network of mRNAs, Long Noncoding RNAs (lncRNAs), and microRNAs (miRNAs). *Med Sci Monit*. 2019;25:1140-54.
 25. Colaprico A, Silva TC, Olsen C, Garofano L, Cava C, Garolini D, et al. TCGAAbiolinks: an R/Bioconductor package for integrative analysis of TCGA data. *Nucleic Acids Res*. 2016;44(8):e71.
 26. Robinson MD, McCarthy DJ, Smyth GK. edgeR: a Bioconductor package for differential expression analysis of digital gene expression data. *Bioinformatics*. 2010;26(1):139-40.
 27. Tremblay M, Viala S, Shafer ME, Graham-Paquin AL, Liu C, Bouchard M. Regulation of stem/progenitor cell maintenance by BMP5 in prostate homeostasis and cancer initiation. *Elife*. 2020;9.
 28. Fan L, Zhu Q, Liu L, Zhu C, Huang H, Lu S, et al. CXCL13 is androgen-responsive and involved in androgen induced prostate cancer cell migration and invasion. *Oncotarget*. 2017;8(32):53244-61.
 29. Pronin A, Slepak V. Ectopically expressed olfactory receptors OR51E1 and OR51E2 suppress proliferation and promote cell death in a prostate cancer cell line. *The Journal of biological chemistry*. 2021;296:100475.
 30. Zhao J, Zhao Y, Wang L, Zhang J, Karnes RJ, Kohli M, et al. Alterations of androgen receptor-regulated enhancer RNAs (eRNAs) contribute to enzalutamide resistance in castration-resistant prostate cancer. *Oncotarget*. 2016;7(25):38551.
 31. Lemos AE, Ferreira LB, Batoreu NM, de Freitas PP, Bonamino MH, Gimba ER. PCA3 long noncoding RNA modulates the expression of key cancer-related genes in LNCaP prostate cancer cells. *Tumour biology : the journal of the International Society for Oncodevelopmental Biology and Medicine*. 2016;37(8):11339-48.
 32. Zhan Y, Jiang L, Jin X, Ying S, Wu Z, Wang L, et al. Inhibiting RRM2 to enhance the anticancer activity of chemotherapy. *Biomedicine & pharmacotherapy = Biomedecine & pharmacotherapie*. 2021;133:110996.